Society For Biomaterials

Characterization and cell behavior of titanium surfaces with PLL/DNA modification via a layer-by-layer technique

Wenli Gao, Bo Feng, Xiong Lu, Jianxin Wang, Shuxin Qu, Jie Weng

Key Laboratory of Advanced Technologies of Materials, Ministry of Education, School of Materials Science and Engineering, Southwest Jiaotong University, Chengdu 610031, China

Received 14 April 2011; revised 19 August 2011; accepted 19 August 2011
Published online 24 May 2012 in Wiley Online Library (wileyonlinelibrary.com). DOI: 10.1002/jbm.a.33238

Abstract: This study describes the fabrication of two types of multilayered films onto titanium by layer-by-layer (LBL) self-assembly, using poly-L-lysine (PLL) as the cationic polyelectrolyte and deoxyribonucleic acid (DNA) as the anionic polyelectrolyte. The assembling process of each component was studied using atomic force microscopy (AFM) and quartz crystal balance (QCM). Zeta potential of the LBL-coated microparticles was measured by dynamic light scattering. Titanium substrates with or without multilayered films were used in osteoblast cell culture experiments to study cell proliferation, viability, differentiation, and morphology. Results of AFM and QCM indicated the progressive build-up of the multilayered coatings. The surface morphology of three types of multilayered films showed elevations in the nanoscale range. The data of zeta potential showed that the surface terminated with PLL displayed positive charge while the surface terminated with DNA displayed negative charge. The proliferation of osteoblasts on modified titanium films was found to be greater than that on control ($p < 0.05$) after 3 and 7 days culture, respectively. Alamar blue measurement showed that the PLL/DNA-modified films have higher cell viability ($p < 0.05$) than the control. Still, the alkaline phosphatase activity assay revealed a better differentiated phenotype on three types of multilayered surfaces compared to non-coated controls. Collectively our results suggest that PLL/DNA were successfully used to surface engineer titanium via LBL technique, and enhanced its cell biocompatibility. © 2012 Wiley Periodicals, Inc. J Biomed Mater Res Part A: 100A: 2176–2185, 2012.

Key Words: titanium, layer-by-layer, poly-L-lysine, DNA, osteoblast

How to cite this article: Gao W, Feng B, Lu X, Wang J, Qu S, Weng J. 2012. Characterization and cell behavior of titanium surfaces with PLL/DNA modification via a layer-by-layer technique. J Biomed Mater Res Part A 2012:100A:2176–2185.

INTRODUCTION

It is well known that the surface properties of a biomaterial, such as surface topography, roughness and chemical composition play a crucial role in success on placement in a biological environment. In particular, activity and behavior of osteoblasts contacting material surface, both *in vitro* and *in vivo*, are influenced by surface properties with precise regard to microtopography and roughness.[1–3] Critical to the long-term success of orthopedic and dental implants is the development of a stable direct connection between bone and surface implant, which must be structural and functional.[4]

Commercial pure titanium (cpTi) and its alloys have been extensively used in dental and orthopedic fields for its excellent biocompatibility, good implant fixation due to the surface reactive oxide, and a high degree of mechanical strength and corrosion resistance.[5,6] However, titanium is only passively integrated with bone and cannot directly bind to bone. The biological performance of implants strongly depends on the first interaction occurring when implant surfaces come into contact with a biological environment.[7] Surface modification is a usual way to control such interaction by modifying the surface properties, such as the chemistry, surface charge, and topography of material surfaces, to enhance bone growth and improve initial stability of bone-contacting implants. The layer-by-layer (LBL) self-assembly technique, described by Decher and Hong[8] in 1991, allows nanoscale control over deposition of a large variety of functional materials in hybrid multilayered films. The electrostatic attraction between positively and negatively charged molecules seems to be a good choice as a driving force for multilayer build up.[9] The multilayer built by the LBL method afford a more stable coating than that prepared by physical adsorption because of the electrostatic attractions between layer-to-layer and layer-to-substrate. The LBL self-assembly of polyanions and polycations into multilayered coatings has emerged as a versatile, inexpensive yet efficient technique to "build" biologically active surfaces in recent years.[10,11]

In this study, LBL self-assembly of poly-L-lysine (PLL) and deoxyribonucleic acid (DNA) was used to fabricate

Correspondence to: B. Feng; e-mail: fengbo@swjtu.edu.cn
Contract grant sponsor: Chinese NSFC; contract grant number: 50871093
Contract grant sponsor: FANEDD; contract grant number: 200554

bioactive coatings on titanium films. PLL is well known not only for its good biocompatibility[12] but also due to its easy conjugation with bioactive molecules.[13,14] This polycation is extensively studied for its applications in drug delivery systems,[15] tissue engineering,[16] microarray glass slide coating,[17] and conjugation with alginate in microencapsulation.[18] PLL is also used in LBL assembly of some negatively charged proteins[19,20] in recent years. PLL is highly charged at neutral pH, and the protonated amino group ($-NH_3^+$) of PLL and the polyanion can be attracted by the ion-pair. So, we chose PLL as the polycation for the assembling on titanium.

DNA, the repository of genetic information with individual-specificity is an intriguing novel coating material for biomaterials. Irrespective of its genetic information, the structural properties of DNA give this unique, natural compound potential for use as a biomaterial coating.[21] Finally, the high-phosphate content in DNA might, via the high affinity of phosphate for calcium ions,[22,23] beneficially affect the deposition of calcium in the bone formation process. The use of DNA as a functional biomaterial, instead as a carrier for its genetic information, has already been used with such as poly(ethylenimine),[24] poly(dimethyldiallylammonium chloride),[25] and poly(allylamine hydrochloride).[26] Ren et al.[27] fabricated DNA films through LBL deposition and released DNA as a DNA delivery system for multilayer films. Only very recently, van den Beucken et al.[21] described the effect of multilayered DNA coating on titanium substrates following the deposition of calcium phosphate and the osteoblast-like cell behavior. So, we chose the LBL coating of titanium prosthesis with PLL/DNA pair and focused on the different bioactivity of every layer terminated with PLL or DNA. In previous work, we have constructed and characterized PLL and DNA multilayered structure via LBL technique, and studied the ability of protein adsorption and biomimetic mineralization of multilayered films on titanium surfaces.[28] The purpose of this study was to evaluate the effect of this PLL/DNA coating on cell viability, cell morphology, and alkaline phosphatase (ALP) activity. The surface characteristics of the LBL implants, including surface morphology and roughness, surface charge and the films thickness, were analyzed by atomic force microscopy (AFM), dynamic light scattering (DLS), and quartz crystal microbalance with dissipation technique (QCM-D), respectively.

MATERIALS AND METHODS

Materials

Commercial pure titanium (cpTi, $\Phi 10 \times 1.5$ mm^2, 99.7%) was gained from Baoji Special Iron and Steel (Shanxi Province, China). PLL (M_W 30–70 kDa), *N*-[2-hydroxyethyl] piperazine-*N*′-[2-ethanesulfonic acid] (HEPEs, free acid, high purity grade) was purchased from Sigma. DNA (fish sperm, sodium salt) was obtained from AppliChem (Germany). All reagents were used as received.

Preparation of titanium surfaces

Titanium disks were burnished with 240, 400, 800, 1500, and 2000 grit silicon carbide paper, washed ultrasonically with distilled water, acetone, ethanol, and distilled water in turn and dried in air at room temperature. Then the samples were immersed in 5*M* NaOH at 80°C for 6 h, rinsed ultrasonically with distilled water for three times, subsequently, dipped in distilled water for 24 h and dried in air. The disks treated above were marked as TiOH.

Preparation of polyelectrolyte multilayer films

The assembling process was according to the previous study.[28] The first layer of PLL was adsorbed onto the Ti surfaces by immersing the titanium substrates in 1 mg/mL PLL/HEPEs buffer (20 m*M* HEPEs, 75 m*M* NaCl, pH 7.4) for 15 min, and then washed with distilled water, dried in air at room temperature. The PLL-covered substrates were then immerged in 1 mg/mL DNA/HEPEs buffer (20 m*M* HEPEs, 75 m*M* NaCl, pH 7.4) for 15 min, then washed and dried. The process of the third layer was repeated as the first layer. These disks were marked as Ti/P, Ti/P/D, and Ti/P/D/P, respectively. All samples were dried in a vacuum desiccator under room temperature for at least 12 h before the measurements. Figure 1 shows the schematic construction of PLL-DNA multilayered films.

Characterization by atomic force microscopy

The roughness of the samples was characterized by AFM (CSPM5000, Being, China) in tapping-mode at ambient temperature. Typical scan sizes were between 10×10 μm^2. Image analysis software (WSxM free software) was used to generate micrographs and quantitatively compare surface roughness, using root mean-square (RMS) calculations, a roughness denotation based on the standard deviations (SD) of the *z*-value (vertical direction).

QCM-D measurement

The QCM-D (USI-System, Japan) was used for the evaluation of the LBL assembly process. As a sensor, titanium-coated QCM-D sensor crystal (14 mm diameter) was used. The titanium sensor crystals were cleaned before measurement in an UV/ozone chamber for 15 min. The crystal resonant frequency (Δf) and the dissipation factor (ΔD) of the oscillator were measured simultaneously at a fundamental resonant frequency (5 MHz) and at a number of overtones, including 35 MHz.

The QCM-D frequency shift was recorded after adsorption of each layer. A change in frequency shift indicates either adsorption or desorption of mass on the resonator surface. Negative frequency shift corresponds to deposition of mass and positive shift indicates removal of mass. The frequency shift (Δf) is related to the adsorbed mass (Δm) according to the Sauerbrey equation.[29] At 5 MHz, a frequency shift of 1 Hz corresponds to a mass change of $\sim$ 17.7 ng/cm^2. This relation is applicable strictly to sufficiently thin, rigid films.[30] A second measurement parameter, dissipation (D), gives qualitative information about the viscoelastic properties of the adsorbed layer.

HEPEs solution was introduced into an axial flow chamber comprising a T-loop to thermally equilibrate the sample at 37 $\pm$ 0.1°C. The sequence of injections into the QCM-D cell

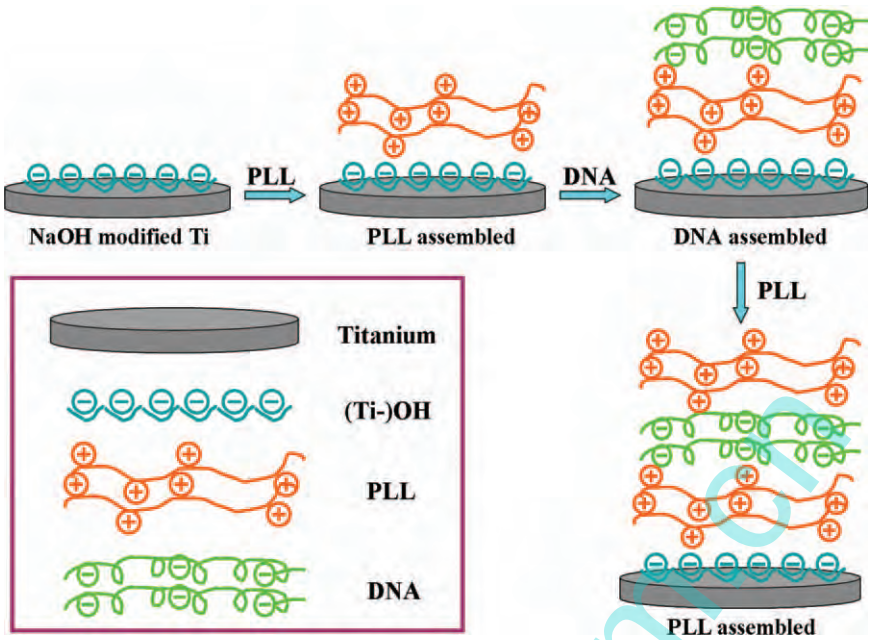

FIGURE 1. Schematic construction of PLL-DNA multilayered films via a LBL technique. [Color figure can be viewed in the online issue, which is available at wileyonlinelibrary.com.]

for an experimental run was as follows: 2 mL of PLL/HEPEs solution, 2 mL of HEPEs solution, 2 mL of DNA/HEPEs solution, 2 mL of HEPEs solution, and 2 mL of PLL/HEPEs solution.

Zeta potential measurements

PLL-DNA multilayers were fabricated on titanium powder nanoparticles (80 nm). The general principle of alternating the surface remains the same as on a flat surface. Surface charges were measured by DLS using a zeta potential analyzer (Nano-ZS90, Malvern Instruments, UK). The mixture of titanium powder nanoparticles and HEPEs buffer (0.1 mg/mL) was agitated using a vortex to disperse the particles uniformly. For multilayers assembling, a polycation solution PLL/HEPEs was added till 1 mL mark to provide sufficient amount of charged species and stored for 15 min (incubation time). The mixture was shaken gently to prevent settling down of the particles and then centrifuged at a speed of 5000 rpm for 10 min. The supernatant was taken out leaving $\sim$ 100 μL of solution in tube to minimize the loss of particles. HEPEs buffer was added till the 1 mL mark, and the particles were redispersed using the vortex mixer. Then a polyanion solution DNA/HEPEs was added and stored for 15 min, shaken, and centrifuged. With that another PLL layer was assembled as described above. Steps from centrifugation to redispersion were repeated three times to wash away additional polyelectrolytes. Results are presented as mean $\pm$ SD from triplicate experiments of three measurements per sample.

Osteoblast culture

Osteoblasts were isolated from neonatal (<1 day old) rat calvarias, using a standard procedure as described previously,[31] after which cells were cryopreserved. Before the initiation of an experiment, cells were thawed and cultured in α-minima essential medium (Gibco), supplemented with 15% v/v fetal bovine serum (FBS, Gibco). All assays were performed with cells of the third culture passage. Before the assays, cells were detached using 0.25% w/v trypsin and 0.05% EDTA solution for 3 min, and at the end of the incubation period, complete culture medium was added to neutralize trypsin and EDTA. Then cells were harvested and centrifuged (5 min, 1200 rpm), resuspended in 500 μL of culture medium and counted using a cell counting plate. Before *in vitro* assays, all samples were sterilized using a UV-irradiation treatment (254 nm; 2 h). Cells were seeded onto titanium substrates (Ti, Ti/P, Ti/P/D, and Ti/P/D/P) with a density of 2×10^4 cells/cm^2 into 24-well plate (Sigma, Aldrich) and incubated at 37°C in 5% CO_2. The culture medium was renewed every two days. All adhesion experiments have been done in triplicate: each experimental point is presented as the mean of three measures on three titanium disks.

Cell viability assay

Cell viability was assessed using a fluorescent indicator dye, Alamar blue. Briefly, at 3 and 7 days after seeding, the medium was aspirated and the cell layer was washed with PBS. And then 300 μL of dye solution (10% v/v FBS/ 10% Alamar blue/ 80% M199) was added to each well, and cells were incubated at 37°C for 4 h. Subsequently, 200 μL of solubilization/stop solution in each well was added into 96-well plates (Sigma). Finally, the absorbance of each well was measured at 570 nm wavelength with an automatic microplate (ELISA) reader (Molecular Devices, Sunnyvale, CA). Measured absorbance values were corrected using three

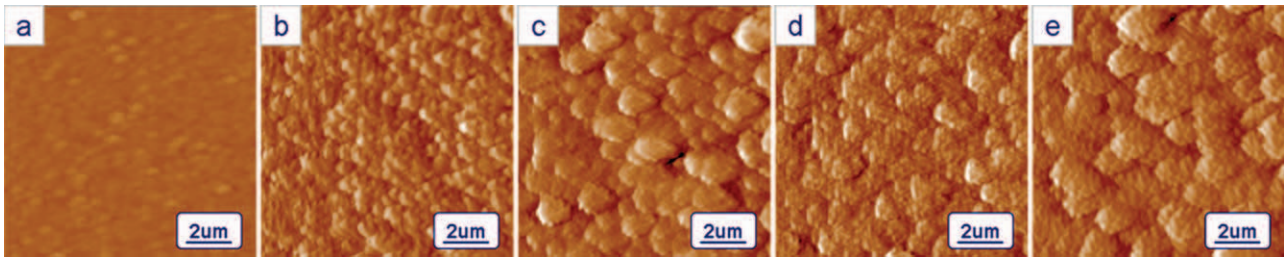

FIGURE 2. AFM tapping mode height images of control and LBL-modified titanium films: (a) control (Ti), (b) TiOH, (c)Ti/P, (d) Ti/P/D, and (e) Ti/P/D/P. [Color figure can be viewed in the online issue, which is available at wileyonlinelibrary.com.]

parallel samples. Normalization of the data was performed to the results of the blank samples. The absorbance of the blank well, which contained no material extracts, was regarded as 100%, and the percentage of absorbance for each well was calculated.

Alkaline phosphatase activity assay

After the selected incubation periods, the samples were washed by PBS and transferred to a new 24-well polystyrene culture plate. About 200 μL of Triton X-100 (1% w/v) was added to each well to make the cells disruption. After incubated in the incubator for 2 h, the 24-well plate was placed into a refrigerator to be frozen at –80°C for 2 h. After running three freeze–thaw cycles to homogenize the solutions, 50 μL of the solutions was used for the ALP activity test. ALP substrate solution (200 μL; 4-NPP, ELPN-500, Bio-Assay Systems) was added to each solution, and the solutions were mixed at room temperature in 3 min. The absorbance of each solution was measured at a wavelength of 405 nm by an ELISA Reader.

Cell morphology

After being cultured for 3 and 7 days, the cells adhered to the samples were washed with PBS. Subsequently, cell fixation was carried out for 12 h at 4°C with 2.5% glutaraldehyde in 0.8*M* PBS. After thorough washing with PBS, the samples were dehydrated using a series of graded ethanol (ethanol/water, v/v, 30, 50, 70, 90, 95, and 100%) and dealcoholized through sequential washings in 50, 70, and 100% ethyl acetate (remainder ethanol, v/v). Finally, the samples were dried using a vacuum desiccator under room temperature for at least 12 h. The samples were sputter coated with gold and examined using scanning electron microscopy (SEM) (FEI Quanta 200, The Netherlands).

The cell-surface interaction was investigated with a fluorescence microscope (DMIL, Leica, Germany). The adhered cells were fixed in 2.5% glutaraldehyde solution in PBS for 10 min at room temperature. The samples were then dipped in Rhodamine123 (Sigma) solution containing 1% PBS for 30 min at room temperature, washed with abundant water, dried, and then measured with a fluorescence microscope.

Statistical analyses

All data were expressed as means ± SD for $n = 3$. Single factor analysis of variance (ANOVA) technique was used to assess the statistical significance of results between groups. The statistical analysis was performed with the software Origin (version 7.0) at a confidence level of 95%.

RESULTS

Atomic force microscopy

Figure 2 shows the AFM height images of control and LBL-coated titanium films. Further analysis of the surface roughness, the RMS roughness values of each sample during the build-up of the films are shown in Table I. The data displayed that the RMS roughness values of the surface with PLL as the outmost layer were significantly higher than that with DNA as the outmost layer, which can explain the different images seen from the Figure 2. Furthermore, the three-dimensional images of the morphology of PLL/DNA multilayered titanium substrates and NaOH-modified titanium are displayed in Figure 3. The modified surfaces showed different morphology and structure from control titanium with a smooth surface (not shown). It was observed that lots of island-like domains on the modified surfaces and the dimensions of the islands showed some difference on each film. Correspondingly, the RMS roughness values changed, as shown in Table I, which agreed with the observation.

QCM-D measurement

The QCM-D measurement whose principle is based on impedance analysis was performed in order to obtain more detailed information about the assembling process. The adsorption of PLL and DNA resulted in a decrease in the normalized frequency and an increase in the dissipation for the overtone 7 as shown in Figure 4. The PLL layer revealed a more rapid frequency decrease than the following layers during 4-h assembling process, which indicates a greater amount of first PLL layer assembled onto the titanium. The frequency change and mass of the outermost-layer of each sample was calculated by the Sauerbrey equation in

TABLE I. Determination of Surface Roughness [RMS (in nm) ± SD]

Samples	RMS ± SD (nm)
Control	9.27 ± 0.5
TiOH	56.4 ± 4.8
Ti/P	41.6 ± 3.2
Ti/P/D	33.2 ± 2.8
Ti/P/D/P	43.9 ± 3.9

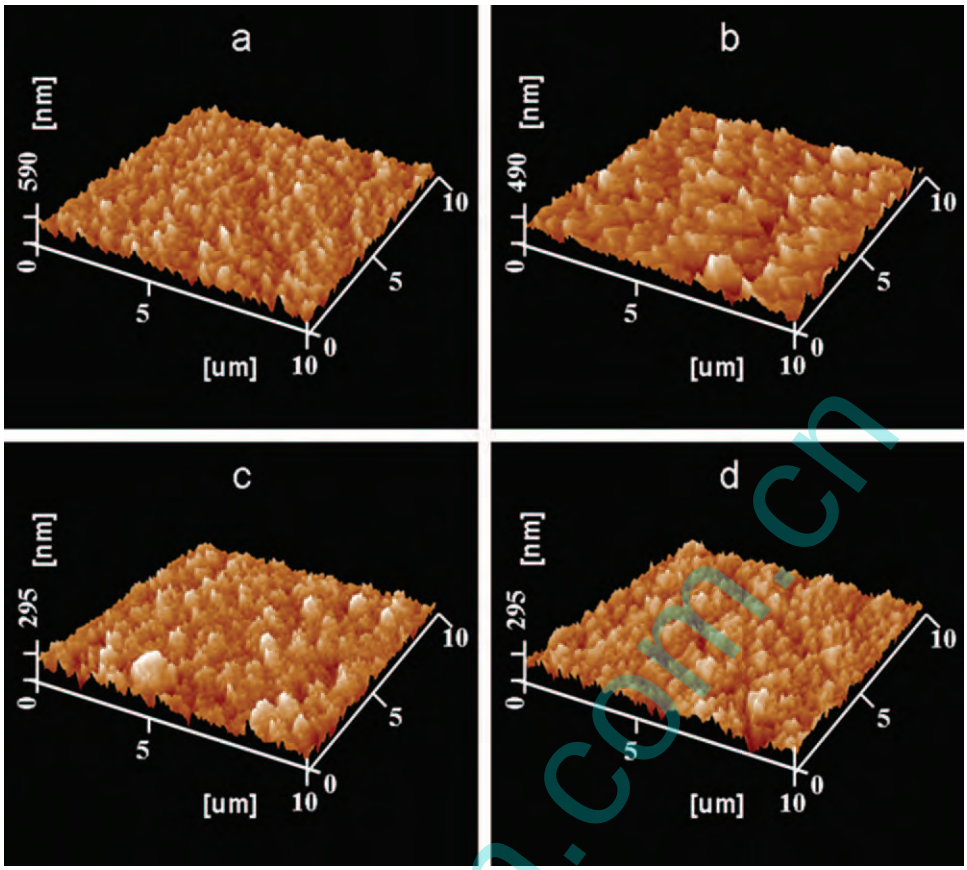

FIGURE 3. Three-dimensional images of the morphology of PLL/DNA multilayered coating on titanium substrates. (a) TiOH, (b)Ti/P, (c) Ti/P/D, and (d) Ti/P/D/P. [Color figure can be viewed in the online issue, which is available at wileyonlinelibrary.com.]

Table II. Figure 5 showed the curves of the mass and thickness of PLL and DNA layer with time in the assembly process. In the figure, it was labeled the absolute values of each assembled layer during the assembling process. The results of mass and thicknesses of each layer measured from QCM (Fig. 5) have been shown to be in good correspondence with data calculated through Sauerbrey equation (see Table II), thus suggesting that relatively uniform monolayers are formed.

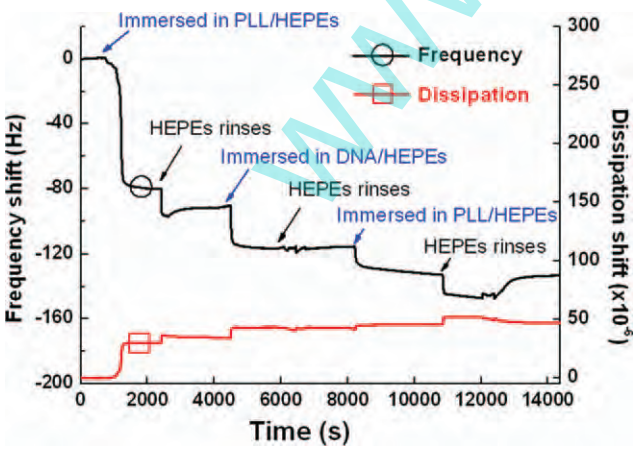

FIGURE 4. Real-time monitoring of the formation of PLL/DNA multilayer films on QCM electrodes in pH 7.4 PLL, DNA, and HEPEs buffer solution. [Color figure can be viewed in the online issue, which is available at wileyonlinelibrary.com.]

Zeta potential measurements

Before the zeta potential measurements, the stepwise growth of the multilayer shells onto titanium nanoparticles at pH 7.4 was monitored by following the diameter changes for the nanoparticles after each deposition step (Fig. 6). Data showed that the sizes of all nanoparticles were in measuring size range of the zeta potential. Figure 7 displayed the variation in the zeta potential for the deposition of PLL/DNA multilayer shells on titanium nanoparticles. The pH of the PLL solutions (in HEPEs buffer at pH 7.4) was lower than the isoelectric point (pI = 9.74) so that PLL brought an excess of positive charges while DNA (pI = 4–4.5) was negatively charged. The control titanium nanoparticles have a zeta potential of -51 ± 4.2 mV. The zeta

TABLE II. Maximal Variations of Frequency and Mass of the Outermost Layer of Each Sample

Samples	$-\Delta f_{max}$ (Hz)	Δm (ng cm^{-2})
Ti/P	83.659 ± 0.195	1485.056 ± 3.461
Ti/P/D	32.057 ± 0.368	569.012 ± 6.532
Ti/P/D/P	20.646 ± 0.513	366.467 ± 9.425

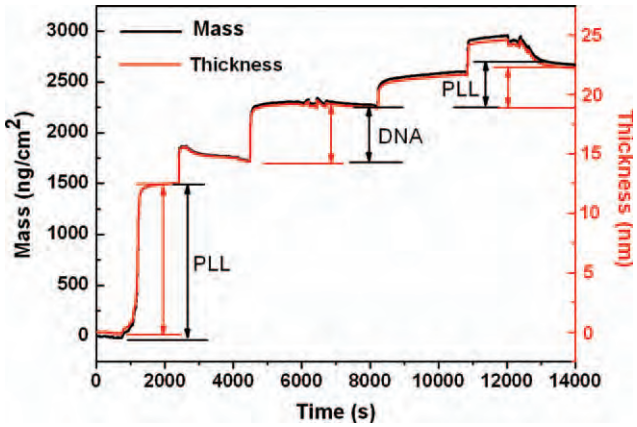

FIGURE 5. The curves of the mass and thickness of each layer with time in the assembly process. [Color figure can be viewed in the online issue, which is available at wileyonlinelibrary.com.]

potential alternated with each new PLL and DNA assembling and became positive (+10 ± 2.1 mV) or negative (-5 ± 5.1 mV) respectively, which indicated that the multilayer surfaces were being charge-overcompensated in each adsorption step thereby facilitating adsorption of the next oppositely charged polypeptide to form the multilayer film onto titanium nanoparticles. These results also illustrated the electrostatic attraction between cationic PLL and anionic DNA.

Cell viability assay

To assess potential effects of multilayered films on cell viability, the mitochondrial redox activity was assessed using Alamar blue assay. Figure 8 shows the values of cell viability on LBL-modified titanium surfaces (Ti/P, Ti/P/D, and Ti/P/D/P) and uncoated titanium surfaces (Ti) after 3 and 7 days incubation, respectively. From the figure, it can be seen, along with the time the number of cells of each sample surface gradually increased, indicating that the property of the sample surface is conducive to cell proliferation. Viability of the cells adhered to the three kinds of LBL-modified titanium films displayed a significant difference ($p < 0.05$) compared to the control sample in this study. To'th et al.[10]

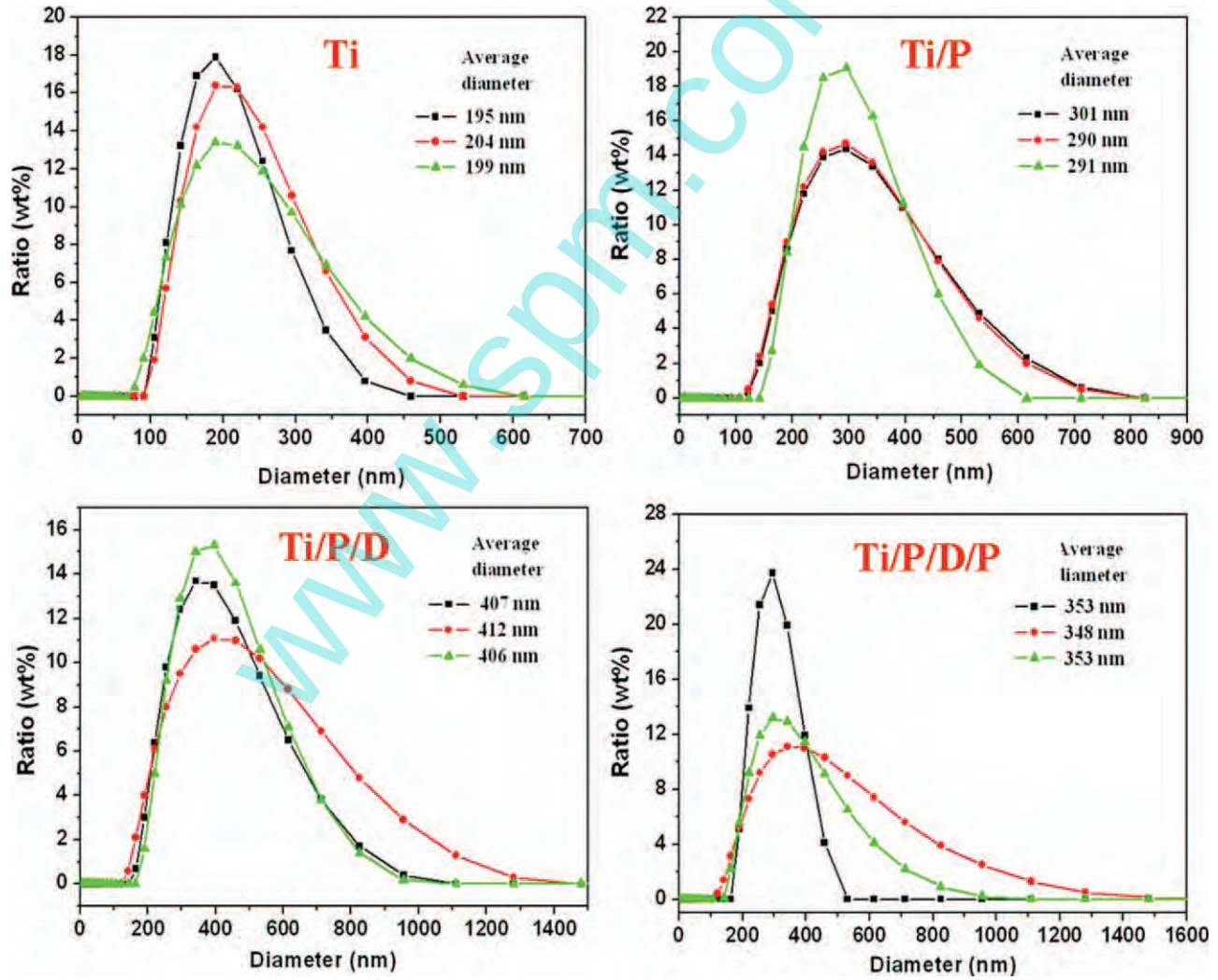

FIGURE 6. Three times measurements of size distribution and the average diameter of titanium nanoparticles modified and control in the HEPEs solution with a concentration of 1.0 mg/mL. [Color figure can be viewed in the online issue, which is available at wileyonlinelibrary.com.]

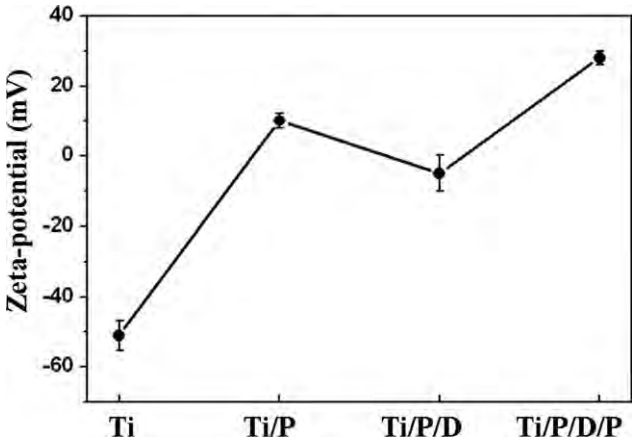

FIGURE 7. Variation in the zeta potential for the deposition of PLL/DNA multilayer shells on titanium nanoparticles. The zeta potential measurements were performed in HEPEs buffer at pH 7.4.

revealed that the terminating layer in polyelectrolyte multilayer films would influence the cell adhesion and cell viability. The result in this study also indicated that PLL or DNA as terminating layer in polyelectrolyte multilayer films is biocompatible and nontoxic for biomedical materials.

ALP activity

ALP activity was used as a biochemical marker for determining osteoblast phenotype and was considered as an important factor in determining bone-forming ability and mineralization.[32] Figure 9 shows ALP activity of cells on LBL-modified titanium films and uncoated titanium films after 7 days. The ALP activity of cells on the three kinds of LBL-modified titanium surfaces was statistically higher than on control surface ($p < 0.05$). This result indicated that, to some extent, ALP activity of osteoblast cells was influenced by LBL modification, and bone-forming ability was enhanced by LBL treatment.

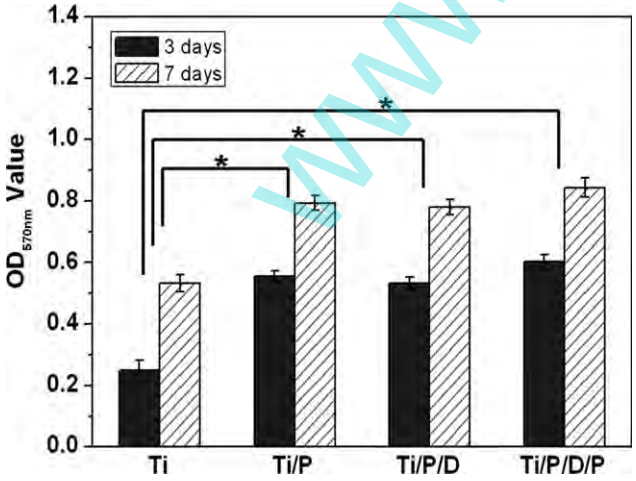

FIGURE 8. Evaluation of cell viability estimated by the Alamar blue assay of osteoblastic cells cultured on Ti/P, Ti/P/D, and Ti/P/D/P titanium substrates after 3 and 7 days incubation, compared with control titanium (Ti), $*p < 0.05$.

Cell morphology

Cell adhesion, spreading, and migration on substrates are the first sequential reactions when coming into contact with a material surface, which is crucial for cell survival. Figure 10 shows the morphology of cells on LBL-modified surfaces and control titanium. After 3 days incubation, cells randomly adhered and spread on both control titanium and LBL-modified titanium, without preferred directions. Osteoblasts attached on control titanium displayed spindle-like feature morphology [Fig. 10(a)] while that attached on LBL-modified titanium films were fully spread [Fig. 10(b–d)]. After 7 days incubation, osteoblasts cultured on all surfaces were flattened, polygonal in shape, and fully spread, exhibiting multilayer proliferation (Fig. 10). On modified surfaces, cells significantly connected and overlapped, which would eventually lead to a complete confluence and the surfaces were fully covered by a continuous sheet of cells. Qualitatively, the LBL-modified titanium surface is more favorable for the cell attachment than the control titanium.

Figure 11 shows the differences in the initial cell spreading/migration evaluated by the analysis of focal adhesion using actin labeling. Osteoblasts adhered to LBL-modified titanium surfaces were fully spread with many bundles of actin microfilaments [Fig. 11(b–d)]. Cells attached to control titanium film also displayed small focal adhesion and a few thin actin microfilaments [Fig. 11(a)].

DISCUSSION

The aim of this study was to fabricate and characterize PLL/DNA multilayered films via the LBL self-assembly technique. The choice of DNA as the anionic polyelectrolyte relates to the structural properties of the DNA molecule and their potential beneficial effects in implantology rather than to the encoded genetic information. As the cationic polyelectrolyte, PLL was used. In our study, we focused on the role of surface properties of a biomaterial, such as surface topography, roughness, and chemical composition, in success on placement in a biological environment.

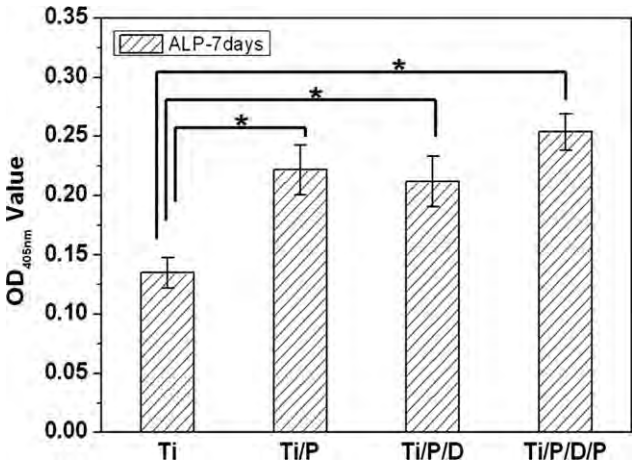

FIGURE 9. Osteoblast alkaline-phosphatase-specific activity after 7 days incubation on Ti/P, Ti/P/D, and Ti/P/D/P titanium surfaces and control titanium (Ti), $*p < 0.05$.

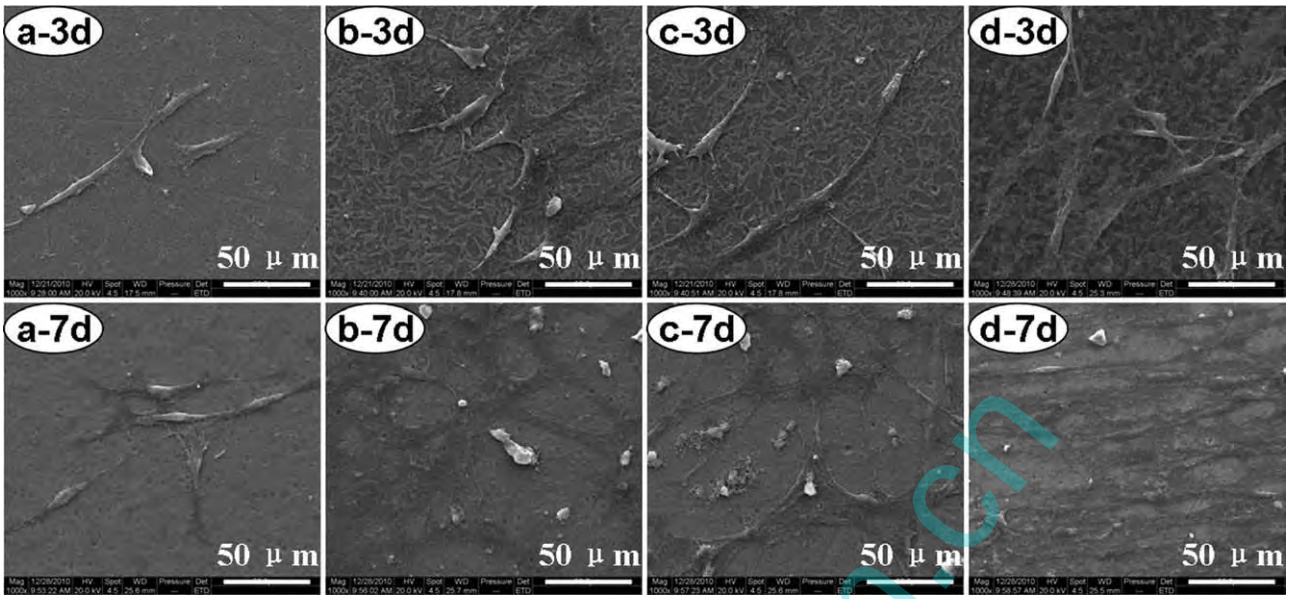

FIGURE 10. SEM images showing the morphology of osteoblasts on samples: (a) Ti, (b) Ti/P, (c) Ti/P/D, and (d) Ti/P/D/P.

The RMS roughness values (Table I) show that, as expected, statistically significant differences in surface roughness are due to the alkali treatment and LBL modified. Furthermore, RMS roughness values of the surface with PLL as the outmost layer were significantly higher than that with DNA as the outmost layer. Shi et al.[33] demonstrated that, in the absence of NaCl, the DNA molecules were lying flat on the PLL layer and only one layer of DNA resided on top of the PLL layer. What's more, NaCl made the DNA strands fold into coiled configurations which should allow a greater number of DNA molecules to pack onto the PLL layer. The gradual growth of the islands was assumed by additional LBL deposition of polyelectrolytes onto islands. This maybe explains the different RMS roughness values between the surface with PLL and DNA as the outmost layer. Rigoberto et al.[34] demonstrated that the roughness and feature size of the multilayer films changed with increasing thickness and that the thicker layers tended to produce larger feature sizes with increased roughness.

QCM-D is a simple and highly sensitive mass sensor by which a wide range of interfacial adsorption reactions can be monitored, on a variety of supports, in real time. The quartz crystal is swept with potential perturbations of different frequencies close to the quartz crystal resonance frequency.[35] This sweep is done as a function of time enabling the measurement of mass changes occurring on the quartz crystal electrode surface. Frequency shift versus time curves (Fig. 4) clearly showed the LBL buildup process of the PLL/DNA coating. With each injection of the PLL or the DNA solution, there was a shift in the crystal frequency, indicating

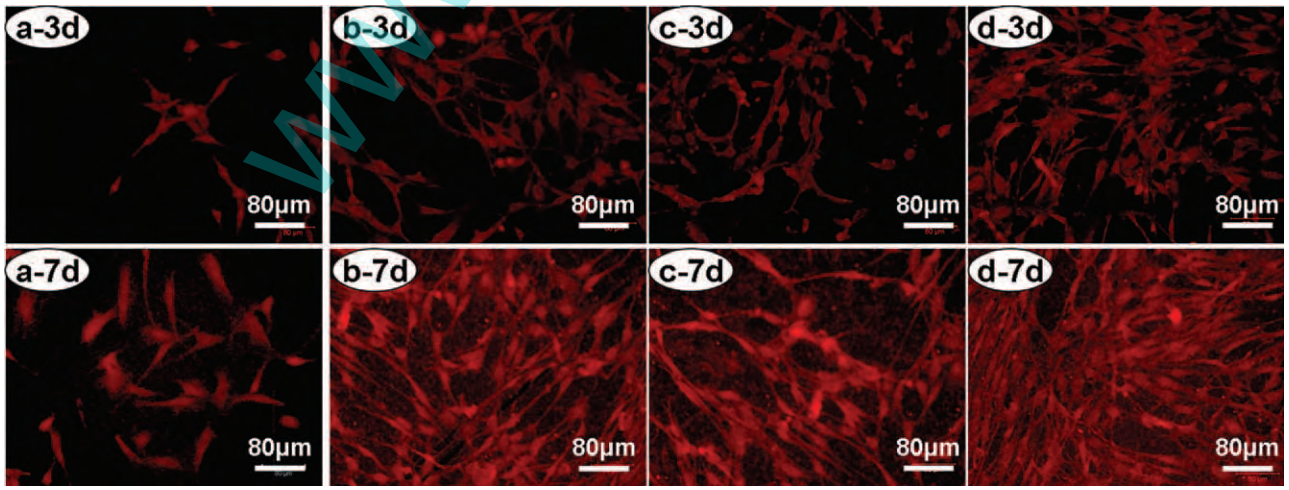

FIGURE 11. Fluorescent light microscopic images of osteoblast cells on samples: (a) Ti, (b) Ti/P, (c) Ti/P/D, and (d) Ti/P/D/P. [Color figure can be viewed in the online issue, which is available at wileyonlinelibrary.com.]

the adsorption mass and thickness of the PLL or the DNA molecules onto the crystal surface (Fig. 5). The ladder form of the QCM traces proved that the LBL structure of the PLL/DNA membrane and the adsorption of PLL and DNA were both stable, since a little frequency shift occurred with the rinsing of the HEPEs buffer. The adsorption of both PLL and DNA were found to be quick as the frequency shift was sharp and coincided with the injection while PLL or DNA would take few minutes to reach equilibrium.

Cell adhesion, spreading, and subsequent proliferation are closely related to the surface properties of the substrate, such as composition, roughness, wettability, and morphology. Anselme et al.[36,37] have suggested that these surface properties have a direct effect on osteoblast attachment, proliferation, and differentiation. We can find that when cells were cultured on thin films of titanium implant materials assembled with PLL or DNA, the effects of material composition were significant. The presence of function groups, amino group (—NH_2), phosphate group (—PO_4), and hydroxyl group (—OH) on the coatings surface, may promote the interaction of materials with bone cells by providing the site for calcium and phosphate nucleation.[38]

Besides chemical composition, it is well known that surface roughness and morphology play an important role in biological responses of biomaterial surfaces.[39] SEM enabled us to highlight intimate contact between cells and concerned biomaterials. Wirth et al.[40] found that the osteoblast adopted three different morphologies. First, the cells are spherical and fix themselves to the substrate by way of thin filopodes. Second, when the cells are well fixed, they remain round and emit flattened cytoplasmic prolongations. Third, when the cells spread, they take on a much flattened form. In our case, osteoblasts also appeared different shapes from spindle-like feature to sheet feature morphology. Osteoblast proliferation is increased for rough surfaces. These results are in agreement with Degasne et al.[41] who found that the cell attachment rates were significantly higher on titanium discs with irregular surfaces.

In addition, we measured the surface charges of titanium powders that modified and noncoated. Electron donor/acceptor character of abiotic surfaces seems to be more easily correlated to cell behavior than pure hydrophobicity.[42] The positively charged PLL and negatively charged DNA may influence the osteoblast cells behavior. But surface charge might not have an obvious effect on cellular adhesion. The results presented here supported that cell adhesion and ALP activity were governed by surface chemistry and roughness. Thus, both surface chemistry and roughness may play important role in determining cell response than the type of topography.

CONCLUSIONS

In our work, PLL and DNA were used to modify the titanium surface by LBL self-assembly technique for the purpose of improving the bone-forming ability of titanium implants. We have demonstrated the successful formation of biocompatible PLL/DNA multilayer films both on planar titanium substrates and titanium nanoparticles. LBL self-assembly using PLL/DNA as the coating pair can successfully improve the bioactivity of titanium surface.

In vitro investigation, both SEM and fluorescence microscopy confirmed that cells adhered to this modified surface have a more flattened morphology and better cell–cell/cell–substrates interactions than that to control titanium. The sample Ti/P/D/P displayed much more amount of cells and much more cells connected and overlapped. Alamar blue and ALP tests also demonstrated the consistent results that such surface engineering and surface roughness were beneficial to improve the cell biocompatibility of titanium implants. Cell adhesion and ALP activity were found to be both governed by surface chemistry and roughness.

REFERENCES

1. Boyan BD, Hummert TW, Dean DD, Schwartz Z. Role of material surfaces in regulating bone and cartilage cell response. Biomaterials 1996;17:137–146.
2. Koontz CS, RampWK, Peindl RD, Kaysinger KK, Harrow ME. Comparison of growth and metabolism of avian osteoblasts on polished disks versus thin films of titanium alloy. J Biomed Mater Res 1998;42:238–244.
3. Frosch KH, Barvencik F, Lohmann CH, Viereck V, Siggelkow H, Breme J. Migration, matrix production and lamellar bone formation of human osteoblast-like cells in porous titanium implants. Cells Tissues Organs 2002;170:214–227.
4. Ramires PA, Romito A, Cosentino F, Milella E. The influence of titania/ hydroxyapatite composite coatings on *in vitro* osteoblasts behaviour. Biomaterials 2001;22:1467–1474.
5. Vercik LCO, Alencar AC, Ramires I, Guastaldi AC. Dental implants: Surface modification of cp-Ti using plasma spraying and the deposition of hydroxyapatite. Mater Sci Forum 2003;416: 669–674.
6. Duran A, Conde A, Coedo AG, Dorado T, Garcia C, Cere S. Sol-gel coatings for protection and bioactivation of metals used in orthopaedic devices. J Mater Chem 2004;14:2282–2290.
7. Caster DG, Ratner BD. Biomedical surface science: Foundations to frontiers. Surf Sci 2002;500:28–60.
8. Decher G, Hong JD. Build-up of ultrathin multilayer films by a self-assembly process: 1. Consecutive adsorption of anionic and cationic bipolar amphiphiles on charged surfaces. Makromol Chem: Macromol Symp 1991;46:321–327.
9. Decher G. Fuzzy nanoassemblies: Towards to layered polymeric multicomposites. Science 1997;277:1232–1237.
10. To'th PT, Vautier D, Haikel Y, Voegel JC, Schaaf P, Chluba J, Ogier J. Viability, adhesion, and bone phenotype of osteoblast-like cells on polyelectrolyte multilayer films. J Biomed Mater Res 2002;60:657–667.
11. Richert L, Lavalle P, Payan E, Shu XZ, Prestwich GD, Stoltz JF, Schaaf P, Voegel JC, Picart C. Layer by layer buildup of polysaccharide films: Physical chemistry and cellular adhesion aspects. Langmuir 2004;20:448–458.
12. Cai D, Kempa K, Ren Z, Carnahan D, Chiles TC. Nanospearing—The biomolecule delivery and its biocompatibility, In: Giersig M, Khomutov GB, editors. Nanomaterials for Application in Medicine and Biology. Dordrecht: Springer Netherlands; 2008. p 81.
13. Mezo G, Remenyi J, Kajtar J, Barna K, Gaal D, Hudecz F. Synthesis and conformational studies of poly(L-lysine) based branched polypeptides with ser and Glu/Leu in the side chains. J Controlled Release 2000;63:81–95.
14. Picart C, Lavalle P, Hubert P, Cuisinier FJG, Decher G, Schaaf P, Voegel JC. Buildup mechanism for poly(l-lysine)/hyaluronic acid films onto a solid surface. Langmuir 2001;17:7414–7424.
15. Smith LC, Duguid J, Wadhwa MS, Logan MJ, Tung CH, Edwards V, Sparrow JT. Synthetic peptide-based DNA complexes for nonviral gene delivery. Adv Drug Deliv Rev 1998;30:115–131.
16. Crompton KE, Goud JD, Bellamkonda RV, Gengenbach TR, Finkelstein DI, Horne MK, Forsythe JS. Polylysine-functionalised

thermoresponsive chitosan hydrogel for neural tissue engineering. Biomaterials 2007;28:441–449.
17. Wu Q, Ma W, Shi R, Zhang B, Mao X, Zheng W. An activated GOPS-poly-L-Lysine-coated glass surface for the immobilization of 60mer oligonucleotides. Eng Life Sci 2005;5:466–470.
18. Orive G, Tam SK, Pedraz JL, Halle JP. Biocompatibility of alginate-poly-L-lysine microcapsules for cell therapy. Biomaterials 2006;27:3691–3700.
19. Gergely C, Bahi S, Szalontai B, Flores H, Schaaf P, Voegel JC, Cuisinier FJG. Human serum albumin self-Assembly on weak polyelectrolyte multilayer films structurally modified by pH changes. Langmuir 2004;20:5575–5582.
20. Zhao WH, Zheng B, Haynie DT. A molecular dynamics study of the physical basis of stability of polypeptide multilayer nanofilms. Langmuir 2006;22:6668–6675.
21. Van den Beucken JJJP, Vos MRJ, Thüne PC, Hayakawa T, Fukushima T, OkahataY, Walboomers XF, Sommerdijk NAJM, Nolte RJM, Jansen JA. Fabrication, characterization, and biological assessment of multilayered DNA-coatings for biomaterial purposes. Biomaterials 2006;27:691–701.
22. Tretinnikov ON, Kato K, Ikada Y. *In vitro* hydroxyapatite deposition onto a film surface-grated with organophosphate polymer. J Biomed Mater Res 1994;28:1365–1373.
23. Kamei S, Tomita N, Tamai S, Kato K, Ikada Y. Histologic and mechanical evaluation for bone bonding of polymer surfaces grafted with a phosphate-containing polymer. J Biomed Mater Res 1997; 37:384–393.
24. Sukhorukov GB, Mohwald H, Decher G, Lvov YM. Assembly of polyelectrolyte multilayer films by consecutively alternating adsorption of polynucleotides and polycations. Thin Solid Films 1996;284:220–223.
25. Pei RJ, Cui XQ, Yang XR, Wang EK. Assembly of alternating polycation and DNA multilayer films by electrostatic layer-by-layer adsorption. Biomacromolecules 2001;2:463–468.
26. Jiang SG, Chen XD, Liu MH. The pH stimulated reversible loading and release of a cationic dye in a layer-by-layer assembled DNA/PAH film. J Colloid Interface Sci 2004;277:396–403.
27. Ren KF, Ji J, Shen JC. Construction and enzymatic degradation of multilayered poly-L-lysine/DNA films. Biomaterials 2006;27: 1152–1159.
28. Gao WL, Feng B, Ni YX, Yang YL, Lu X, Weng J. Protein adsorption and biomimetic mineralization behaviors of PLL–DNA multilayered films assembled onto titanium. Appl Surf Sci 2010;257: 538–546.
29. Sauerbrey G. Use of vibrating quartz for thin film weighing and microweigh2 ing. Z Phys 1959;155:206–222.
30. Rodahl M, H.o. ok F, Fredriksson C, Keller CA, Krozer A, Brzezinski P, Voinova M, Kasemo B. Simultaneous frequency and dissipation factor QCM measurements of biomolecular adsorption and cell adhesion. Faraday Discuss 1997;107:229–246.
31. Ishaug SL, Yaszemski MJ, Bizios R, Mikos AG. Osteoblast function on synthetic biodegradable polymers. J Biomed Mater Res 1994; 28:1445–1453.
32. Price PA. Vitamin K-dependent formation of bone Gla protein (osteocalcin) and its function. Vitam Horm 1985;42:65–108.
33. Shi XY, Sanedrin RJ, Zhou FM. Structural characterization of multilayered DNA and polylysine composite films: Influence of ionic strength of DNA solutions on the extent of DNA incorporation. J Phys Chem B 2002;106:1173–1180.
34. Rigoberto A, Park M, Baba A, Kaneko F. Photoalignment in ultrathin films of a layer-by-layer deposited water-soluble azobenzene dye. Langmuir 2003;19:654–665.
35. Meng S, Liu ZJ, Shen L, Guo Z, Chou LSL, Zhong W, Du QG, Ge JB. The effect of layer-by-layer chitosan-heparin coating on the endothelialization and coagulation properties of a coronary stent system. Biomaterials 2009;30:2276–2283.
36. Anselme K, Bigerelle M, Noel B, Ruderman I, Hardouin P, Iost A. Improvement in the morphology of surfaces for cell adhesion. Eur Cells Mater 1 2001;2:35–48.
37. Anselme K, Bigerelle M, Noel B, Iost A, Hardouin P. Effect of grooves titanium substratum on human osteoblastic cell growth. J Biomed Mater Res 2002;60:529–540.
38. Feng B, Weng J, Yang BC, Qu SX, Zhang XD. Characterization of surface oxide films on titanium and adhesion of osteoblast. Biomaterials 2003;24:4663–4670.
39. Zhu X, Chen J, Scheideler L, Reichl R, Geis-Gerstorfer J. Effects of topography and composition of titanium surface oxides on osteoblast responses. Biomaterials 2004;25:4087–4103.
40. Wirth C, Comte V, Lagneau C, Exbrayat P, Lissac M, Jaffrezic-Renault N, Ponsonnet L. Nitinol surface roughness modulates *in vitro* cell response: A comparison between fibroblasts and osteoblasts. Mater Sci Eng C 2005;25:51–60.
41. Degasne I, Lesourd M, Hure G, Basle MF, Chappard D. Measurement of titanium roughness by contact profilometry and image analysis. Implantodontie 1997;27:29–39.
42. Yang Y, Tian J, Deng L, Ong JL. Morphological behavior of osteoblast-like cells on surface-modified titanium *in vitro*. Biomaterials 2002;23:1383–1389.